Supporting Information

Vacancy-Cluster-Mediated Surface Activation for Boosting CO_2 Chemical Fixation

Wenxiu Liu [a]‡, Lei Li [a]‡, Wei Shao [a]‡, Hui Wang [a], [b] *, Yun Dong [c], Ming Zuo [a], Jiandang Liu [c], Hongjun Zhang [c]*, Bangjiao Ye [c], Xiaodong Zhang [a], [b]* and Yi Xie [a], [b]

[a] Hefei National Research Center for Physical Sciences at the Microscale, University of Science and Technology of China, Hefei, 230026, P. R. China.

[b] Institute of Energy, Hefei Comprehensive National Science Center, Hefei, 230031, China.

[c] State Key Laboratory of Particle Detection and Electronics, University of Science and Technology of China, Hefei, Anhui 230026, P. R. China

Experimental section:

Preparation of bulk FeOCl.

Bulk FeOCl was prepared according to a conventional chemical-vapor transition method.[1] In detail, Fe_2O_3 and $FeCl_3$ (AR, Sinoreagent, China) with atom radio of 1:1.3 were mixed with fully grinding, and then sealed in a glass tube. The tube was heated at 653 K for 5 days, with a ramp rate of about 3 K per minute for both the heating and cooling processes. The product was ground and washed with acetone (AR, Sinoreagent, China) for several times to remove excess $FeCl_3$, and then dark purple powders were obtained.

Preparation of FeOCl nanosheets with Fe-Cl vacancy cluster.

Typically, 60 mg of bulk FeOCl powder was soaked in cyclohexane solution of n-butyllithium under an inert atmosphere. After 8 h, the powder was collected, and washed with cyclohexane and ethanol for several times. The powder was then dispersed in 100 ml of distilled water, and sonicated in ice water for 30 min. The brown red product was filtered, washed with distilled water and ethanol, and dried under vacuum. The product was stored under an inert atmosphere for further characterization.

Preparation of FeOCl nanosheets with single Cl vacancy.

Typically, 60 mg of bulk FeOCl powder was soaked in acetonitrile solution under 1 MPa CO_2 (CEL-KPR, Beijing China Education Au-light Technology Co., Ltd.). After 6 h, the powder was washed with ethanol and dried under vacuum. The product was stored under an inert atmosphere for further characterization.

Catalytic tests of CO_2 cycloaddition with epoxides.

Typically, 5 mg of FeOCl nanosheets powders dispersed in 5 ml of N, N-Dimethylformamide (DMF) and then 200 μL of propylene oxide (PO) were added in the dispersions which were transferred into reactor. The reactor was filled with 0.3-MPa CO_2 at room temperature. The reaction proceeded under stirring with specific temperature for 6 h, then cooled down to room temperature. The liquid products were analyzed by NMR using $CDCl_3$ as solvent and 1,1,2,2-tetrachloroethane as the internal standard on a Bruker 400 MHz NMR spectrometer. Theoretical yield of propylene carbonate (PC) = mol of propylene carbonate / mol of epoxide × 100 %. (Because of the volatility of PO, the calculation result is small)

Characterization.

X-ray diffraction (XRD) were performed on a Philips X'Pert Pro Super diffractometer with Cu Kα radiation (λ=1.54178 Å). Raman spectra were recorded on a RenishawRM3000 Micro-Raman system, in which the excitation wavelength of 532 nm. The scanning electron microscopy (SEM) images were obtained on a JEOL JSM-6700F SEM. The transmission electron microscopy (TEM) images were taken on H-7650 (Hitachi, Japan) operated at an acceleration voltage of 100 kV. High-resolution transmission electron microscopy (HRTEM) and energy dispersive spectroscopy (EDS) mapping analyses were carried out on a Talos F200 TEM/STEM with a spherical aberration corrector. X-ray photoelectron spectra (XPS) were acquired on an ESCALAB MK II with Mg Kα as the excitation source. The nitrogen absorption and desorption curves were recorded on a Tristar II 3020M. Atomic force microscopy (AFM) measurement was performed by means of Veeco DI Nanoscope Multi Mode V system. The Fourier-

transform infrared (FT-IR) spectra were acquired on a NICOLET FT-IR spectrometer in a KBr tablets, scanning from 4000 to 400 cm^{-1} at room temperature. Fe contents were determined by the inductively coupled plasma atomic emission spectroscopy (ICP-AES) (Thermo Fisher iCAP 7400). Electron Probe Microanalyzer (EPMA) were carried out on EPMA-8050G (Shimadzu, Japan).

Positron annihilation spectroscopy.

The positron annihilation lifetime measurements were performed at room temperature using a digital spectrometer (TechnoAP, Japan) with a time resolution of around 200 ps in FWHM. The powders were compressed at approximately 8 MPa into two pellet-shaped samples in the size of ϕ10 × 1 mm. The positron source (^{22}NaCl, ∼30 μCi, sealed by two Kapton polyimide foils in the size of 10 mm × 10 mm × 7.5 μm) was sandwiched between two identical pellet-shaped samples. The sample-source-sample set was sandwiched by an Al foil and fixed in a vacuum chamber which was evacuated by a turbo molecular pump. Each spectrum was collected to the total counts of more than 4×106 with a counting rate of around 200 counts/s. The total channel number is 8192, and the channel width is 10.417 ps/channel.

In-Situ DRIFTS measurements: *In-situ* diffuse reflectance infrared Fourier-transform spectroscopy (DRIFTS) measurements were obtained by using a Bruker IFS 66v Fourier-transform spectrometer equipped with a Harrick diffuse reflectance accessory at the Infrared spectroscopy and microspectroscopy beamline (BL01B) in National Synchrotron Radiation Laboratory (NSRL) in Hefei, China.

DFT calculation details.

The present spin-polarized first principle DFT calculations are performed by Vienna Ab initio Simulation Package (VASP)[2-4] with the projector augmented wave (PAW)[5] method. The exchange-functional is treated using the generalized gradient approximation (GGA) of Perdew-Burke-Ernzerhof (PBE)[6] functional. The energy cutoff for the plane wave basis expansion was set to 450 eV and the force on each atom less than 0.02 eV/Å was set for convergence criterion of geometry relaxation. 4×4 supercell of Single-layer FeOCl (010) with different defects (pure, Cl vacancy and Fe-Cl dimmer vacancy) were used for simulation. The Brillouin zone integration were performed using 2×2×1 k-point sampling for all systems. The self-consistent calculations apply a convergence energy threshold of 10^{-5} eV. The van der Waals interaction was considered by using the DFT-D3 method.[6] Transition state searching was performed using the climbing-image nudged elastic band (CI-NEB) method.[7]

Supplementary figures and tables

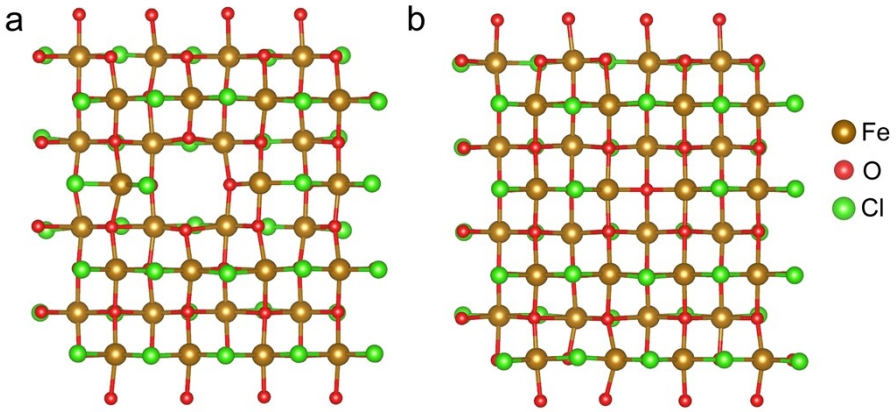

Figure S1. Theoretical models of FeOCl slabs containing (a) Fe-Cl vacancy cluster and (b) Cl vacancy.

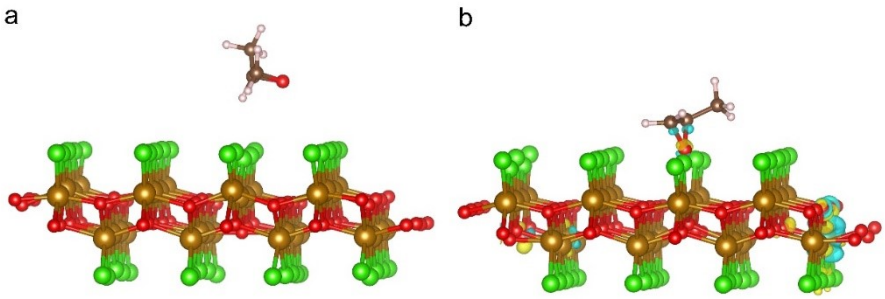

Figure S2. The charge densities of PO molecules absorption of onto (a) pristine FeOCl slab and (b) FeOCl slab with Cl vacancy.

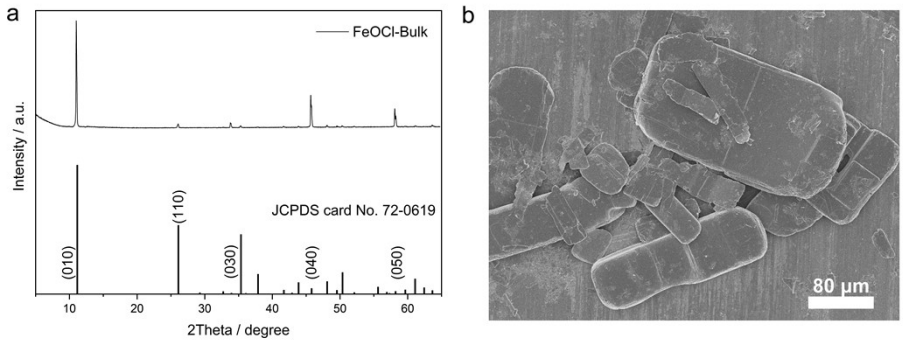

Figure S3. (a) XRD pattern and (b) SEM image of FeOCl bulk.

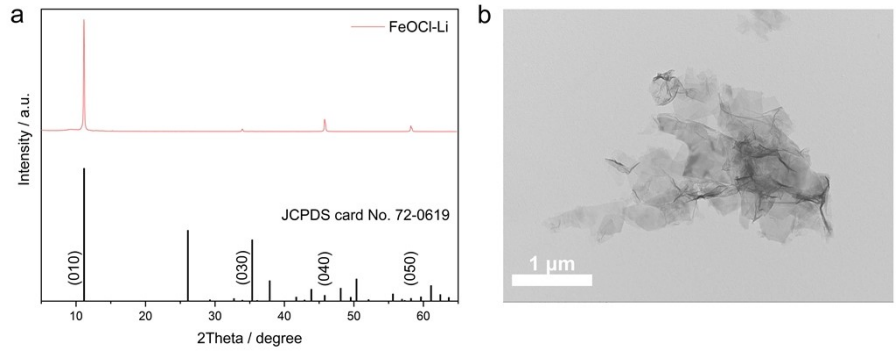

Figure S4. (a) XRD pattern and (b) TEM image of FeOCl-Li nanosheets.

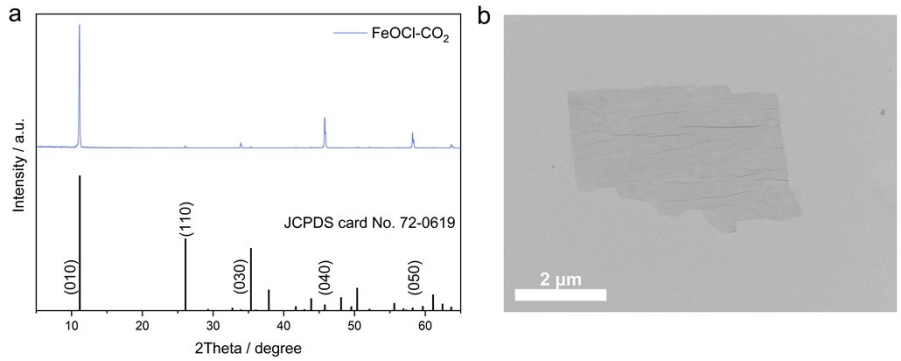

Figure S5. (a) XRD pattern and (b) TEM image of FeOCl-CO_2 nanosheets.

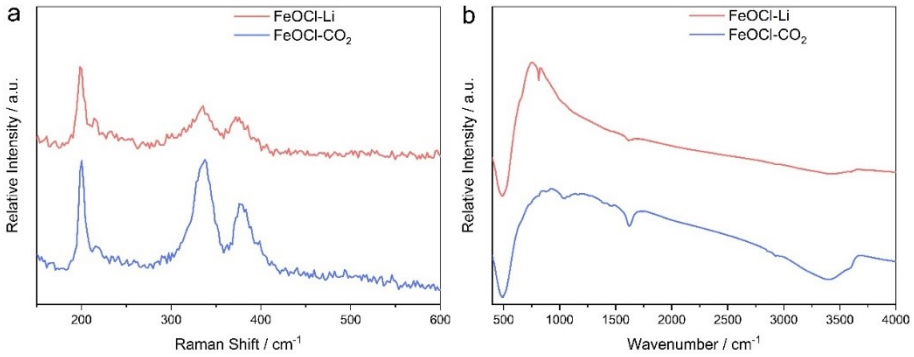

Figure S6. (a) Raman spectra and (b) FTIR spectra of FeOCl-CO_2 nanosheets and FeOCl-Li nanosheets.

The nearly similar Raman spectra (**Figure S6a**) of two samples further proved that the structure has no changed. Almost identical peaks located at 330 cm^{-1} and 199 cm^{-1} could be assigned to the characteristic peaks of FeOCl and the Fe-Cl bond, respectively.[8, 9] As displayed in **Figure S6b**, in detail, the bond at 500 cm^{-1} was typical Fe-O bond and the broad peaks at 3400 cm^{-1} and 1615 cm^{-1} can be assigned to adsorbed water on the surface and hydroxyl group, respectively.[10]

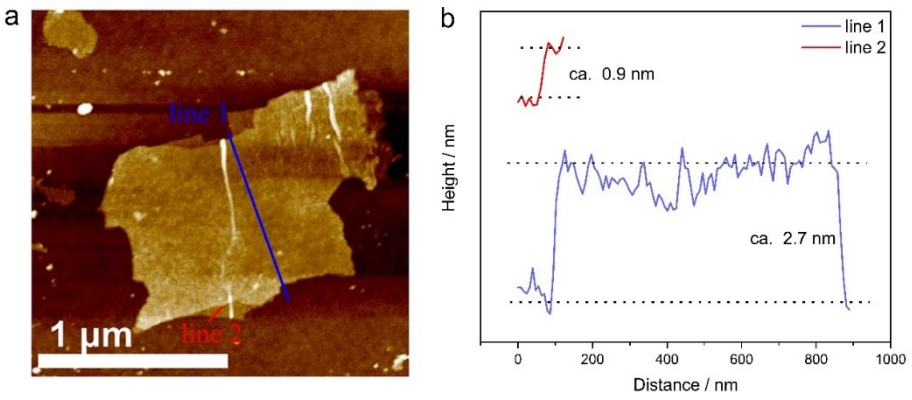

Figure S7. (a) AFM image and (b) the corresponding height profiles of FeOCl-CO_2 nanosheets.

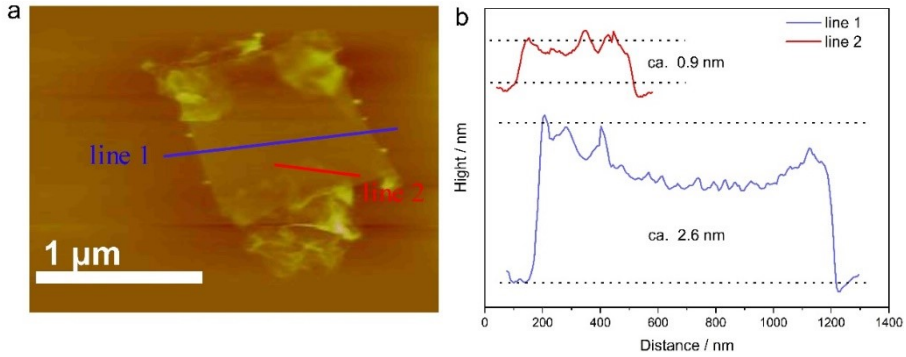

Figure S8. (a) AFM image and (b) the corresponding height profiles of FeOCl-Li nanosheets.

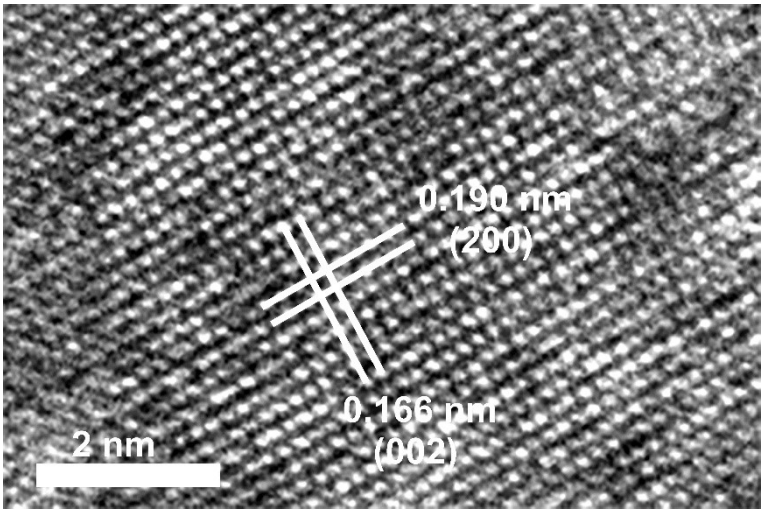

Figure S9. HRTEM of FeOCl-CO_2 nanosheets.

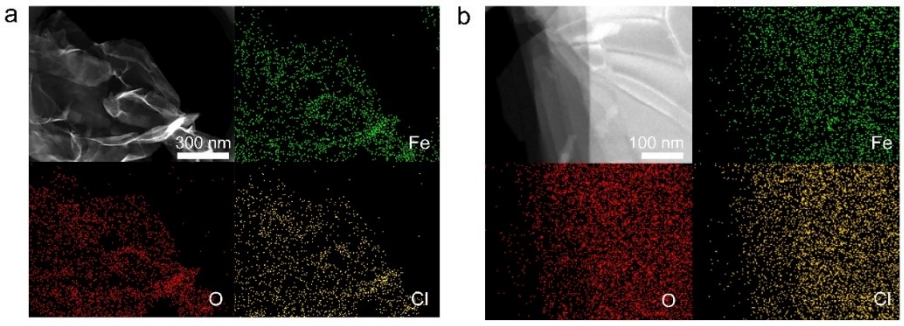

Figure S10. STEM image and corresponding EDS mapping images of(a) FeOCl-Li nanosheets and (b) FeOCl-CO_2 nanosheets.

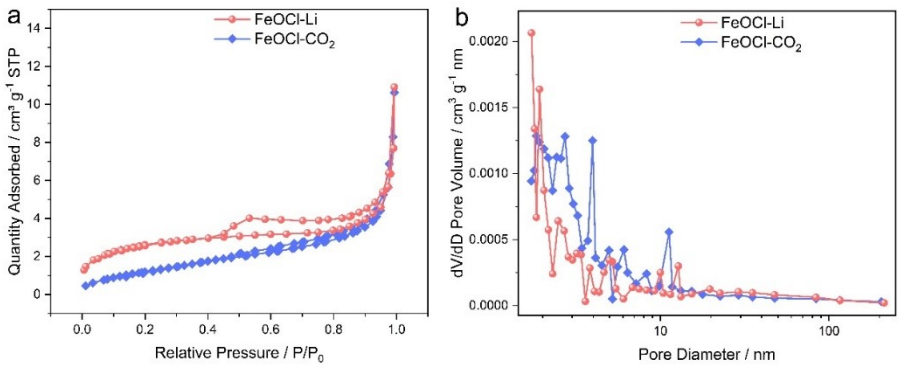

Figure S11. (a) N_2 adsorption isotherms and (b) mesopores size distributions of different FeOCl nanosheets.

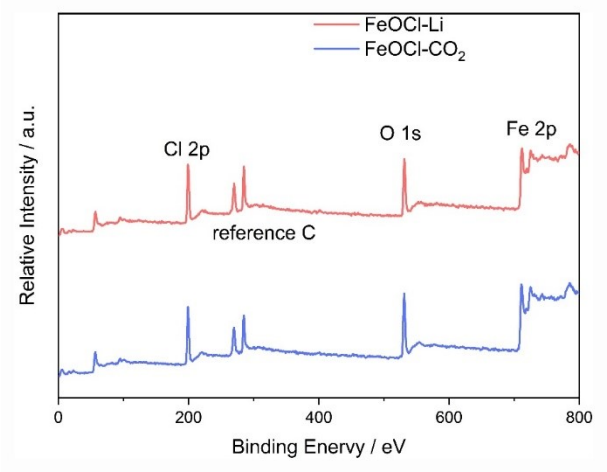

Figure S12. XPS survey spectra of FeOCl-CO_2 and FeOCl-Li nanosheets.

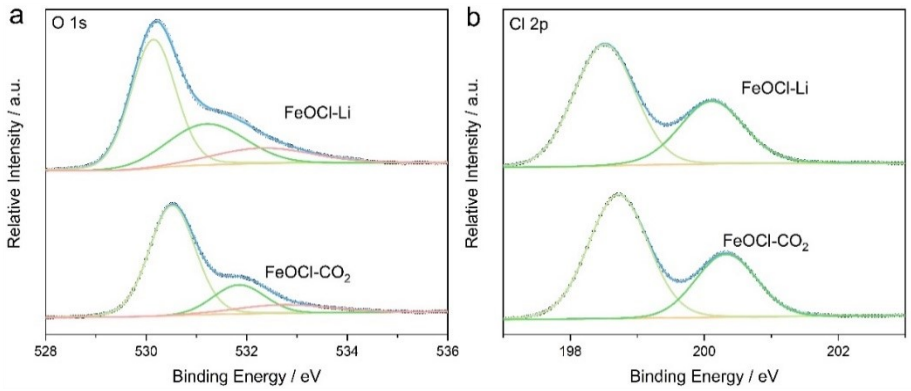

Figure S13. XPS spectra of(a) O 1s and (b) Cl 2p.

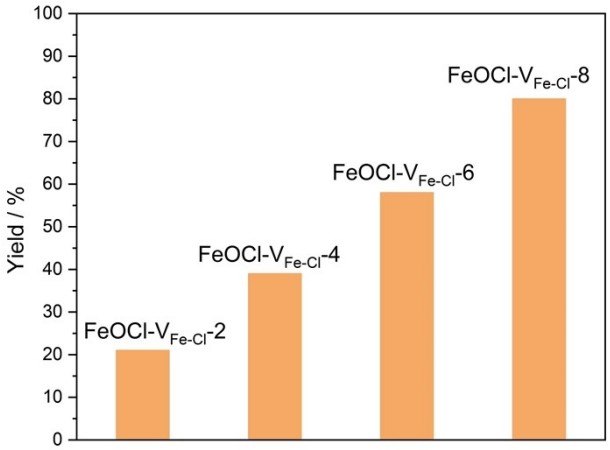

Figure S14. The yields of propylene carbonate with FeOCl-V_{Fe-Cl} nanosheets with different intercalation time under 0.3-MPa of CO_2 at 423K.

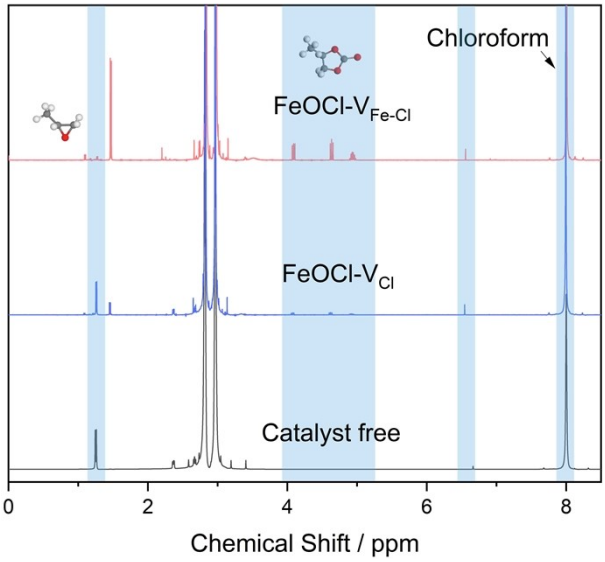

Figure S15. Representative NMR spectra of synthetic PC from the reaction of CO_2 and PO in DMF solution.

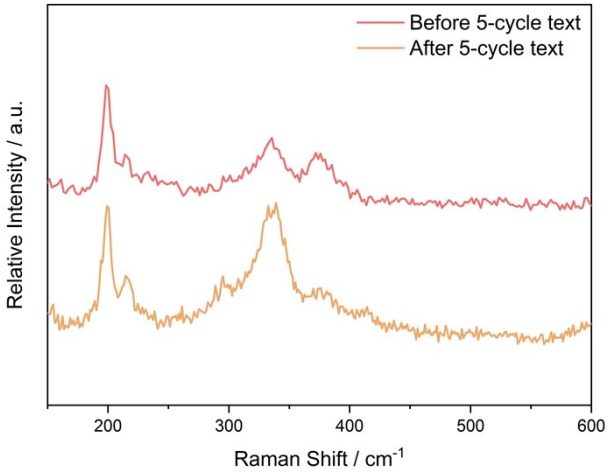

Figure S16. Raman spectra before (red) and after (orange) 5-cycles catalytic tests for the FeOCl-V_{Fe-Cl} nanosheets.

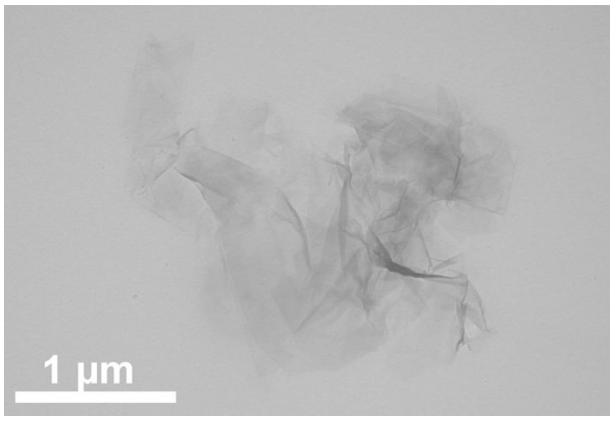

Figure S17. TEM images after 5-cycles catalytic tests for the FeOCl-$V_{Fe\text{-}Cl}$ nanosheets.

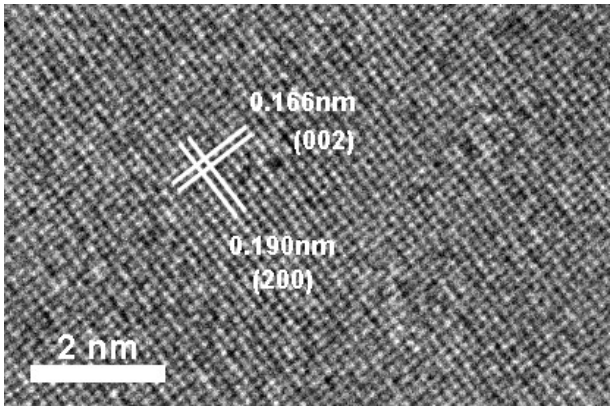

Figure S18. HRTEM images after 5-cycles catalytic tests for the FeOCl-$V_{Fe\text{-}Cl}$ nanosheets.

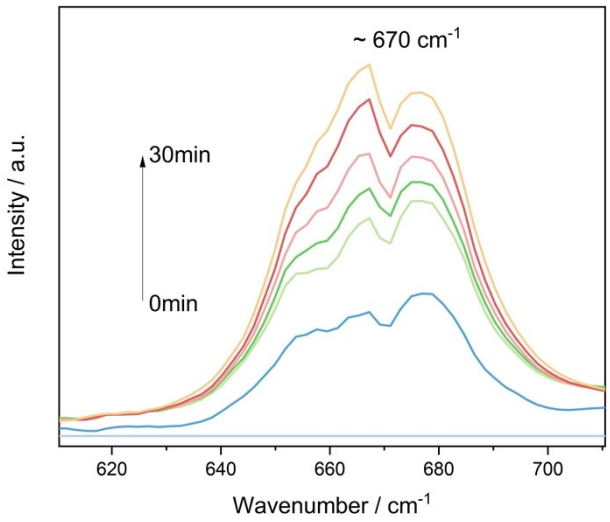

Figure S19. *In-situ* DRIFTS spectra for the FeOCl-V_{Fe-Cl} with CO_2 and PO.

Table S1. Positron Annihilation Lifetime Parameters of FeOCl-CO_2 and FeOCl-Li nanosheets

Sample	τ_1 (ps)	τ_2 (ps)	τ_3 (ns)	I_1 (%)	I_2 (%)	I_3 (%)
FeOCl-CO_2	249.0±10.0	374.0±8.0	1.6±0.1	40.4±5.2	58.5±5.2	1.1±0.1
FeOCl-Li	228.0±3.0	408.0±3.0	2.3±0.1	43.1±1.1	55.0±1.1	2.0±0.1

Table S2. Calculated Positron Annihilation Lifetime Values of FeOCl nanosheets

Defect	Free	V_{Fe}	V_O	V_{Cl}	V_{Cl-O}	V_{Fe-Cl}	V_{Fe-O}
Lifetime (ps)	250.8	264.1	289.1	361.3	365.1	431.8	314.4

Table S3. Elemental compositions of the FeOCl-V_{Fe-Cl} nanosheets with different intercalation times (ICP results)

Catalyst	Fe / wt%
Bulk FeOCl	48.3
FeOCl-V_{Fe-Cl}-2	46.5
FeOCl-V_{Fe-Cl}-4	45.1
FeOCl-V_{Fe-Cl}-6	42.4
FeOCl-V_{Fe-Cl}-8	38.3

Table S4. Elemental compositions of the FeOCl-V_{Fe-Cl} nanosheets with different intercalation times (EPMA results)

Catalyst	Fe / Mol%	Cl / Mol%
Bulk FeOCl	34.1	33.8
FeOCl-V_{Fe-Cl}-2	33.2	31.2
FeOCl-V_{Fe-Cl}-4	33.1	29.2
FeOCl-V_{Fe-Cl}-6	32.7	28.9
FeOCl-V_{Fe-Cl}-8	32.4	27.4

ICP-AES and EPMA were employed to measure their elemental content of FeOCl-V_{Fe-Cl} synthesized by different intercalation times. In the ICP measurement, nitric acid is used to dissolve the samples. Since the presence of nitrate ions affected the accuracy of the elemental Cl content, EPMA determines the elemental Cl content. Based on **Table S3**, Fe element was ca. 38.3 wt% detected by the inductively coupled plasma atomic emission spectroscopy (ICP-AES). According to the results of the EPMA in **Table 4**, it was surprising to find that the elemental content of Fe and Cl gradually decreased with the increasing of the synthesis time, proving the increase of the defect concentration. The excess O maybe absorbed O_2 or water. The elemental content of Fe It is concluded that the actual stoichiometric ratio of FeOCl-V_{Fe-Cl} is $Fe_{0.81}OCl_{0.69}$.

References:

1. X. J. Yang, X. M. Xu, J. Xu and Y. F. Han, *J. Am. Chem. Soc.*, 2013, **135**, 16058-16061.
2. G. Kresse, J. Furthmüller and J. Hafner, *Phys. Rev. B*, 1994, **50**, 13181.
3. G. Kresse and J. Furthmüller, *Phys. Rev. B*, 1996, **54**, 11169.
4. G. Kresse and J. Furthmüller, *Comput. Mater. Sci.*, 1996, **6**, 15-50.
5. G. Kresse and D. Joubert, *Phys. Rev. B*, 1999, **59**, 1758.
6. J. P. Perdew, K. Burke and M. Ernzerhof, *Phys. Rev. Lett.*, 1996, **77**, 3865.
7. G. Henkelman, B. P. Uberuaga and H. Jónsson, *J. Chem. Phys.*, 2000, **113**, 9901-9904.
8. Y. Zeng, P. Gu, Z. Zhao, B. Zhang, Z. Lin, Y. Peng, W. Li, W. Zhao, Y. Leng and P. Tan, *Adv. Mater.*, 2022, 2108847.
9. J. Zhang, G. Liu and S. Liu, *New J. Chem.*, 2018, **42**, 6896-6902.
10. T. Yu, X. Zhao, L. Ma and X. Shen, *Mater. Res. Bull.*, 2017, **96**, 485-490.